MODIS TEB calibration algorithm improvements for future L1B collection

Tiejun Chang[a*], Ashish Shrestha[a], Carlos Perez Diaz[a], Yonghong Li[a], Na Chen[a], Aisheng Wu[a], and Xiaoxiong Xiong[b]

[a] Science Systems and Applications, Inc., Lanham, MD 20706
[b] Sciences and Exploration Directorate, NASA/GSFC, Greenbelt, MD 20771

Abstract

Terra and Aqua MODIS have provided continuous global observations for scientific applications for more than 20 and 18 years, respectively. The radiometric calibration of the MODIS thermal emissive bands (TEB) is based on a quadratic approximation of the instrument response. The calibration coefficients look-up tables (LUTs) are updated using the response of the MODIS on-board blackbody (BB) with the response background subtracted by space view. The quarterly on-board BB warm-up and cool-down activity temperature ranges from 270 K to 315 K, and the derived offset has a relatively large uncertainty. Electronic cross-talk, an artifact that affects both instrument calibration and Earth view (EV) radiance retrievals, is corrected based on lunar observations. Calibration assessments using EV observations (e.g. ocean, desert, Antarctic Dome Concordia, and deep convective clouds) provide useful information to evaluate the impact of the Terra safe mode (February 2016) and Aqua MODIS formatter reset (January 2018) events on both MODIS instruments. This study focuses on the TEB radiometric calibration algorithm improvements for future collections based on calibration assessments using EV measurements and analytical modeling. Measurement stability and consistency over specific Earth scenes with a wide temperature range, as well as their brightness temperature (BT) dependency, are used for bias estimations in the calibration coefficients. Calibration coefficients are derived and updated after adjusting the current fitting algorithm. Thereafter, using the test LUTs, their impact on the Level 1B (L1B) data for different EV scenes is analyzed.

Keywords: MODIS, radiometric calibration, TEB, DCC, Dome-C

1. INTRODUCTION

The Moderate Resolution Imaging Spectroradiometer (MODIS) instruments on-board NASA's Terra and Aqua satellites have been continuously operating for 20 and 18 years, respectively; well beyond their designed lifetimes of 6 years [1-4]. MODIS has provided continuous global observations and produced an unprecedented amount of science data products with primary applications for studies of the Earth's land, ocean, and atmosphere[5-9]. MODIS has 36 spectral bands, where bands 1 to 19 and 26 are reflective solar bands (RSB) covering a wavelength range from 0.41 µm to 2.1 µm, and bands 20 to 25 and 27 to 36 are thermal emissive bands (TEB) with wavelengths ranging from 3.8 µm to 14.2 µm. The onboard solar diffuser and blackbody (BB), along with lunar observations and Earth view (EV) measurements, are used for post-launch calibrations. After 20 years of on-orbit operation, the electronic cross-talk amongst Terra MODIS TEB 27 to 30 has increased substantially; causing biases in the EV brightness temperature (BT) measurements and impacting their stability. The electronic cross-talk between these bands has been characterized and corrected using lunar measurements. Moreover, the cross-talk correction coefficients obtained from these lunar observations are updated regularly to maintain the accuracy of the Collection 6.1 (C6.1) Level 1B (L1B) product, especially for the increasing electronic cross-talk contamination in the photovoltaic (PV) longwave infrared (LWIR) bands[10].

The MODIS TEB on-orbit calibration, performed with an on-board BB and a space view (SV), uses a quadratic response function. During the quarterly-scheduled warm-up and cool-down (WUCD) events, the BB temperature varies from 270 K to 315 K. The instrument's non-linear coefficient and offset terms, which are derived using the WUCD data, are updated (as needed) following the look-up table (LUT) delivery procedure[11, 12]. Due to the challenges associated with the accurate determination of the offset coefficient in the response function using these on-orbit WUCD calibrations, the C6.1 algorithm handles offset coefficient for each mirror side differently for Terra MODIS and continues to rely on pre-launch offset coefficients for Aqua MODIS. To assess the impact of the offset's uncertainty, cold targets can be used to assess the calibration's bias and consistency. From these assessments, the effect of major instrument response changes is analyzed, and based on these analysis, we provide calibration algorithm and LUT delivery improvements for future L1B product. This paper focuses on the analyses of the MODIS TEB calibration algorithm improvements. Cold targets (i.e. Dome Concordia (Dome-C) and deep convective clouds (DCC)) are used for these assessments.

2. BACKGROUND

2.1 MODIS TEB calibration algorithm

MODIS has 16 TEB that cover the mid-wave infrared (MWIR: bands 20-25) and LWIR (bands 27-36) spectral regions. The TEB detectors are located on two cold focal plane assemblies (CFPAs): a short-wave and mid-wave infrared (SMIR) FPA and a LWIR FPA. The CFPA is temperature-controlled on-orbit at 83 K using a passive radiative cooler to have a stable detector gain. Each TEB consists of 10 detectors. Bands 20-30 are PV, while bands 31-36 are photoconductive (PC). An on-board calibrator BB serves as the primary calibration source, while the SV provides a reference for the instrument background. The BB temperature is controlled using a heater and is measured using a set of 12 uniformly-distributed thermistors. The Terra MODIS BB nominal temperature was set to 290 K originally, and changed to 285 K after the WUCD event on April 25, 2020. The Aqua BB nominal temperature is 285 K. The MODIS TEB calibration uses a quadratic calibration algorithm on a scan-by-scan basis for each TEB detector and side of the scan mirror[1-4, 11, 12].

The BB WUCD is used to characterize the instrument's non-linear response coefficients on-orbit. The BB WUCD is a quarterly event with a temperature varying from instrument ambient temperature (about 270 K) to 315 K. The linear coefficient of the response function for each TEB is calculated scan-by-scan using the non-linear coefficient and offset terms[11, 12].

The MODIS TEB calibration is based on a quadratic algorithm that converts the instrument digital response to calibration radiance (L_{CAL}). The calibration radiance from the BB is adjusted for instrument's internal thermal-emission due to response-versus-scan-angle (RVS) effects,

$$L_{CAL} = RVS_{BB}\varepsilon_{BB}L_{BB} + (RVS_{SV} - RVS_{BB})L_{SM} + RVS_{BB}(1-\varepsilon_{BB})\varepsilon_{cav}L_{cav}\ , \qquad (1)$$

where ε is the emissivity from different sources and L are the radiances from the BB, scan mirror (SM), and cavity (cav). The second term on the right-hand side of Eq. (1) defines the scan mirror emission effect, while the third term is the BB reflection of the cavity emission.
A quadratic function is used for instrument response calibration[11, 12],

$$L_{CAL} = a_0 + b_1 dn_{BB} + a_2 dn_{BB}^2. \qquad (2)$$

The terms a_0, b_1, and a_2 are calibration coefficients. The linear term dominates the radiance calculation. The dn_{BB} is the instrument digital output after subtracting the background signal from the SV. The quadratic algorithm is applied during the WUCD calibrations, scan-by-scan linear coefficient calculations, and EV retrievals. The digital responses of the Terra MODIS PV LWIR and PC TEB are electronic and optical cross-talk corrected and used for the WUCD calibrations, linear coefficient calculations, and Earth radiance retrievals for C6.1. The RVS and ε were determined during pre-launch, whereas the a_0, a_2, and the band 21 b_1 coefficients are updated quarterly (as needed) using on–board BB WUCD measurements.

2.2 MODIS TEB Collection 6.1

Section 2.1 provided the general algorithm for calibration of instrument response. The current C6.1 LUT update algorithms for Terra and Aqua MODIS are summarized in Table 1 by following certain procedure[13]. The Band 21 b_1 is derived using BB CD data with the offset and non-linear terms constrained to zero in the fitting algorithm (not shown in Tables 1 and 2). The Terra PC LWIR TEB cross-talk coefficients were derived using lunar observation analyses from the beginning of the mission[12].
An electronic cross-talk correction is applied to Terra MODIS PV LWIR bands 27-30 during calibration and EV retrievals. Brightness temperature difference analyses between the current LUT and newly-derived a_0 and a_2 coefficients are performed. If the update criteria exceed, a LUT update is issued. To evaluate the cross-talk effect on the BT changes, a

semi-L1B test is performed to include both the cross-talk induced scene and BT dependencies. The mini-L1B and semi-L1B tools, used for the simulation of the algorithm improvement assessments, will be presented in detail in Sec. 3.1.

Table 1. Terra and Aqua MODIS C6.1 calibration algorithm.

<table>
<tr><th rowspan="2">Band</th><th>Aqua</th><th colspan="2">Terra</th></tr>
<tr><th>Calibration algorithm</th><th>Calibration algorithm</th><th>Cross-talk correction</th></tr>
<tr><td>20</td><td rowspan="9">PL a_0
PL adjusted CD a_2</td><td rowspan="9">$a_{0\_ms1} = 0$
$a_{0\_ms2} = a_{0\_ms2}^{free\text{-}fit} - a_{0\_ms1}^{free\text{-}fit}$
CD a_2</td><td rowspan="5">Electronic cross-talk Corrections for selected detectors recommended for future improvement</td></tr>
<tr><td>22</td></tr>
<tr><td>23</td></tr>
<tr><td>24</td></tr>
<tr><td>25</td></tr>
<tr><td>27</td><td rowspan="4">PV LWIR electronic cross-talk</td></tr>
<tr><td>28</td></tr>
<tr><td>29</td></tr>
<tr><td>30</td></tr>
<tr><td>31</td><td rowspan="2">a_0=0, CD a_2</td><td rowspan="6">$a_0 = 0$
CD a_2</td><td></td></tr>
<tr><td>32</td><td rowspan="5">PC LWIR optical cross-talk</td></tr>
<tr><td>33</td><td rowspan="4">a_0=0
PL adjusted CD a_2</td></tr>
<tr><td>34</td></tr>
<tr><td>35</td></tr>
<tr><td>36</td></tr>
</table>

2.3 Assessment using Earth scenes

As previously discussed in Sec. 2.1., the biases estimated from Earth scene measurements can be used to evaluate the MODIS calibration. Typical scenes used for the TEB calibration assessment include: Dome-C, ocean, desert, and DCC[13-23]. The broad BT coverage of these scenes is useful for the evaluation of the BT and scene dependencies. Dome-C and DCC are cold targets normally used for the assessment of the offset term in the calibration algorithm. Dome-C, located at 75.12 S, 123.39 E, is one of the most homogeneous and stable EV targets. The site is in a high polar plateau region with a mean elevation of 3200 meters near the Italian-French base of Concordia. Its relative uniformity, long-term stability, dry atmosphere, low aerosol loading and wind speed, low cloud cover, and frequent satellite overpasses make it a useful site to track the calibration stability and consistency of satellite sensors, especially for the on-orbit calibration of thermal remote sensing satellite instruments[23-26]. For each selected granule in the study, the radiances from a 20 km x 20 km region-of-interest are retrieved and converted to BT.

DCC are extremely cold bright targets that are near-Lambertian at low solar and view zenith angles. These scenes are normally used for RSB stability assessments due to their consistent reflectance in the visible and near infrared spectrum, and minimal amount of water vapor and aerosols when viewed from space. These are also suitable for sensor calibration and inter-comparisons between satellite sensors[18-20]. The DCC pixel identification and selection in this work followed the procedure described in References 18 and 19. The DCC pixels are identified as those located over the tropical domain - between latitudes 30° N and 30° S - with BTs lower than 205 K at 11 µm (MODIS TEB 31). Spatial homogeneity thresholds are used to characterize the DCC core. The IR temperature and visible reflectance (0.65-µm; MODIS band 1) standard deviations were computed over all 3 km x 3 km blocks surrounding each potential DCC pixel. Afterwards, if the IR temperature standard deviation (STD) was higher than a 1 K threshold, or the reflectance STD larger than 3 %, the potential DCC pixel was discarded. DCC and quasi-DCC (qDCC) measurements, developed for the assessment of the TEB in our previous work, are also used to demonstrate a normalization technique and compare with other EV scenes[13, 14]. Only nighttime measurements are analyzed. However, as presented in our previous work, using daytime DCC have constraints over the calibration assessment of the MWIR bands; thus the nighttime quasi-DCC technique is used. Examination of the visible reflectance homogeneity is ignored due to a lack of reflectance measurements.

The ocean site, located in the North Atlantic Ocean (23.70 N, 41.57 W), and the Libya-4 desert (28.55 N, 23.39 E) provide uniform scenes for a large BT range that covers most of the typical BTs for most TEB. As presented in Sec. 2.1, the large uncertainty of the offset in the calibration equation is an issue. Thus, cold scenes assessments (e.g. DCC/qDCC and Dome-C) are used for calibration improvements. However, the ocean and desert scenes can be used for the verification of the analytical modeling and correction effect over higher BTs - especially to evaluate the results at typical temperatures. Both scenes consist of selected regions that are 20 km x 20 km in size. The inter-comparison between MODIS and other reference sensor is also applied for the assessment. For example, the comparison between Aqua MODIS and Atmospheric Infrared Sounder (AIRS) instrument on Aqua spacecraft is also used for calibration assessments in this paper.

In this paper, the mirror side differences at low BTs are used to assess the performance of the offset coefficient in the calibration algorithm. Mirror side difference is defined as the difference between mirror side 2 and mirror side 1 BT measurements. Scene uniformity and number of samples are important to enhance the analysis' accuracy. Dome-C, the ocean, and desert provide good uniformity, while DCC/qDCC provide sufficient samples per month for statistical analyses.

3. CALIBRATION ASSESSMENT AND IMPROVEMENT

3.1 Analytical modeling

From the MODIS TEB calibration algorithm presented in Sec. 2.1, the calibration uncertainty impact on the L1B product can be analytically-derived with first order approximation[13, 14]. The major calibration errors include: BB emissivity uncertainty, BB temperature measurement bias, and uncertainties in the non-linear and offset coefficients. These uncertainties propagate to the linear coefficient b_1, and with the first order effect, the b_1 uncertainty can be derived.
From the EV retrieval equation, the impact on the EV radiance retrieval can be derived from the offset, non-linear, and linear coefficients' uncertainties. Hence, the calibration uncertainty effect has strong BT dependence. For cold targets (low EV radiance), the offset term yields the dominant effect. This analytical modeling can also be used to assess the calibration bias from Earth scene measurements[13, 14]. One practical application is to use it to evaluate mirror side and detector differences, or assess long-term stability using the same target. Thus, the calibration uncertainty impact on the L1B product can be modeled.
In this paper, the analytical modeling is used to evaluate the Terra and Aqua MODIS TEB mirror side differences and derive corrections for the biases. Because the EV scenes used in this analysis are DCC and Dome-C, it is assumed that the bias comes from the offset term for these low BT scenes. The analytical modeling is also used for the verification of the application of the derived offset correction to warm scenes (i.e. desert and ocean).

3.2 Terra MODIS

3.2.1 Terra safe mode impact

The Terra spacecraft entered into safe mode on February of 2016 (02/18/2016: 14:33:17Z) during an inclination adjust maneuver. This caused MODIS to enter into safe mode as well, resulting in the nadir and space view doors closing. The spacecraft was successfully recovered from safe mode back into science mode on 02/22/2016, and the key telemetry temperatures (i.e. BB, instrument, electronic, and CFPA) were stabilized after day 02/27/2016. A gain change was observed for most detectors, along with increased noise levels. A WUCD calibration was performed from 03/02/2016 to 03/05/2016, and a LUT with updated QA and calibration coefficients (a_0, a_2) was delivered on 03/10/2016 (2016/070). The 2016 Terra MODIS safe mode event caused a large impact on response and stability that translated onto the calibration coefficients and noise equivalent temperature difference (NEdT) for the LWIR TEB[24-26]. Overall, the event had a large impact on the electronic cross-talk between PV LWIR TEB 27-30[10].

As discussed previously, the safe mode event caused instrument response changes[27-29]. Hence, because the MODIS TEB LUT delivery procedure uses the one-year moving average window to reduce seasonal fluctuation, the LUT one year after safe mode was affected by the calibration before the event. This issue can be revealed by analyzing the discontinuity in the mirror side differences before and after safe mode. The Terra MODIS safe mode event had a significant impact on the PV LWIR TEB 27-30 mirror side differences - likely due to the LUT update. Because the Terra TEB LUT update uses a yearly moving sliding window average and the safe mode event caused rapid instrument response changes, the LUT update did not catch these changes until year 2017 (marked using the vertical green dashed line). Figure 1 shows the PV LWIR TEB mirror side differences over the entire Terra MODIS mission for DCC scenes. Band 27 exhibits the largest mirror side difference (1.8 K) after the safe mode event, while the other three bands show a mirror side difference smaller than 1 K. After the LUT was updated to catch the instrument response changes, the mirror side differences gradually decrease. This effect can cause biases at all scenes. For the cold scenes, these biases are related to the offset coefficient from the LUT. The offset term's effect on these biases decreases as the scene's BT increases. The Dome-C (75.10° S, 123.39° E) and ocean (23.7° N, 41.57° W) mirror side differences are used to verify the offset term's bias impact on higher BT scenes. Band 30 shows that its mirror side differences became larger in the opposite direction a few years after the safe mode event and recently came back. The cause of the TEB 30 mirror side differences, along with its bias, is under investigation.

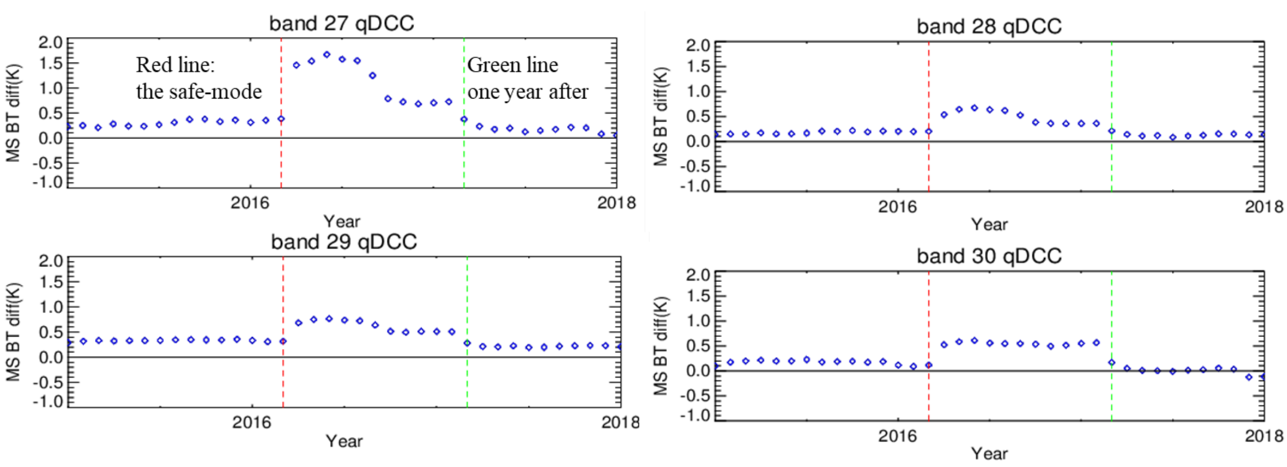

Figure 1. (Left) Terra LWIR bands 27-30 mirror side differences long-term trending using qDCC. Each symbol represents the monthly-averaged mirror side difference. The vertical red dashed line indicates the time occurrence for the safe mode event (February 2016), while the green line represents exactly one year after. (Right) Mirror side differences from one year before to two years after safe mode.

The Terra MODIS safe mode effect on PC LWIR bands 33-36 is different from the other two band groups. The PC LWIR TEB mirror side differences are much smaller than those from PV LWIR bands 27-30. However, these mirror side differences show less stability and appear to be impacted by the safe mode event in a different way. As shown in Fig. 2, the mirror side PV LWIR TEB mirror side differences are due to the fact that the LUT did not follow the rapid instrument response changes. Nonetheless, after one year, the mirror side differences decreased substantially.

3.2.2 Terra MODIS calibration improvement

Assessments of MODIS TEB measurements over Earth scenes can be used for calibration algorithm improvements. It was revealed from the mirror side difference analysis (using DCC and other Earth scenes) that the safe mode-induced instrument response changes have an effect on the yearly moving average window used to produce the calibration coefficients that are delivered whenever there is a LUT update. Thus, it affects the L1B products for one year after the safe mode event. A calibration and LUT delivery improvement is proposed to adjust the moving average period and avoid crossing the safe mode timeline.

Figure 2 displays the official C6.1 LUT offset terms (blue) and the proposed improvements for a future Collection (red) for the safe mode-impacted Terra PV LWIR TEB 27-30 from 2014 to 2020. Each marker represents the band-averaged LUT value. The vertical dashed lines indicate the time of occurrence for the safe mode (February 2016) and one year after the event. Figure 3 shows the official C6.1 LUT non-linear coefficients (blue) and the proposed improvements for a future Collection (red) for the Terra PV LWIR TEB 27-30 from 2014 to 2020. Each symbol defines the band-averaged LUT value.

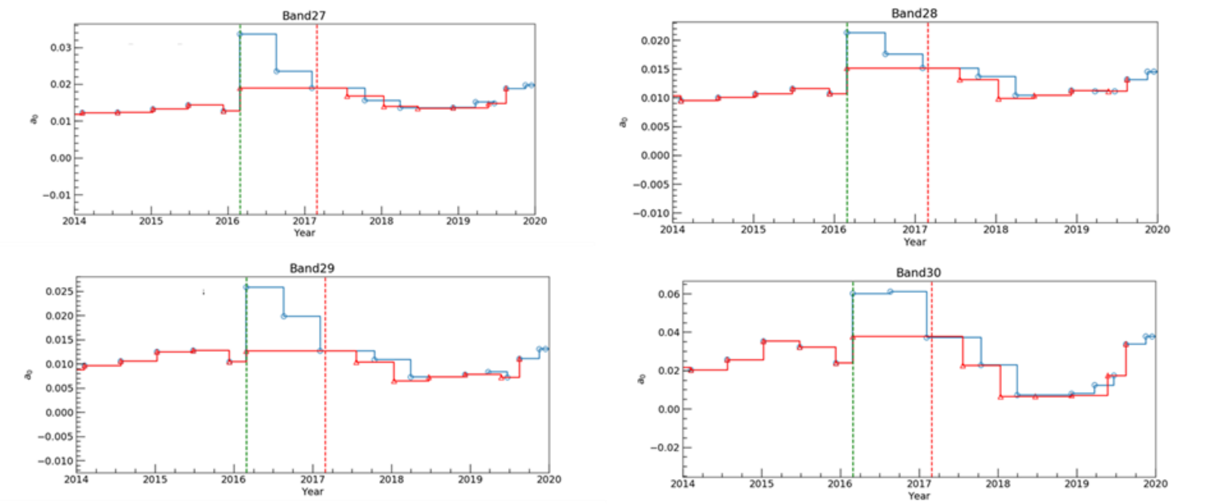

Figure 2. Official C6.1 LUT offset terms (blue) and the proposed improvements for a future Collection (red) for the safe mode-impacted Terra PV LWIR TEB 27-30 from 2014 to 2020. Each marker represents the band-averaged LUT value. The vertical dashed lines indicate the time of occurrence for safe mode (February 2016) and one year after the event.

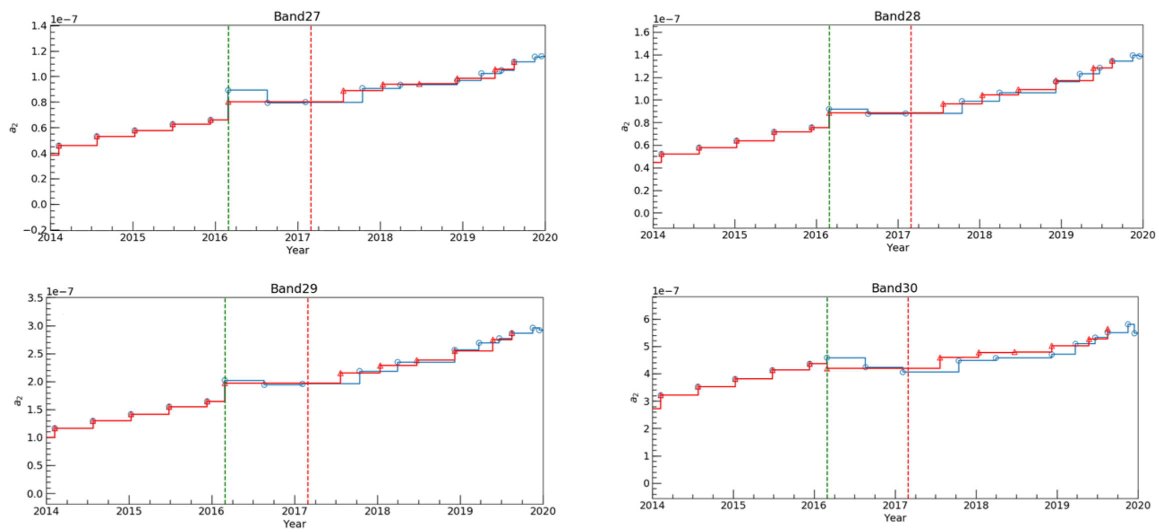

Figure 3. Official C6.1 LUT non-linear coefficients (blue) and the proposed improvements for a future Collection (red) for the safe mode-impacted Terra PV LWIR TEB 27-30 from 2014 to 2020. Each marker represents the band-averaged LUT value. The vertical dashed lines indicate the time of occurrence for safe mode (February 2016) and one year after the event.

The LUT improvement change is assessed using the semi-L1B tool. Because the impact is significant for low BT scenes, the semi-L1B tests are performed over Dome-C and DCC. Figure 4 shows the Terra PV LWIR 27-30 mirror side BT differences from 2014 to 2020 over Dome-C. Each symbol defines the monthly- and band-averaged value. The blue stars represent C6.1, while the red diamonds indicate future improvements. The vertical dashed lines indicate the time of occurrence for safe mode (February 2016) and one year after the event. Because assessments using DCC require large amount of samples, L1A granules that contain DCC pixels are collected (and processed using the semi-L1B tool) for one month after the safe mode event. Table 2 lists the DCC mirror side BT differences for the same month (March 2016) using C6.1 and the future improvements Collection. Significant reductions in mirror side BT differences validate the proposed LUT improvement.

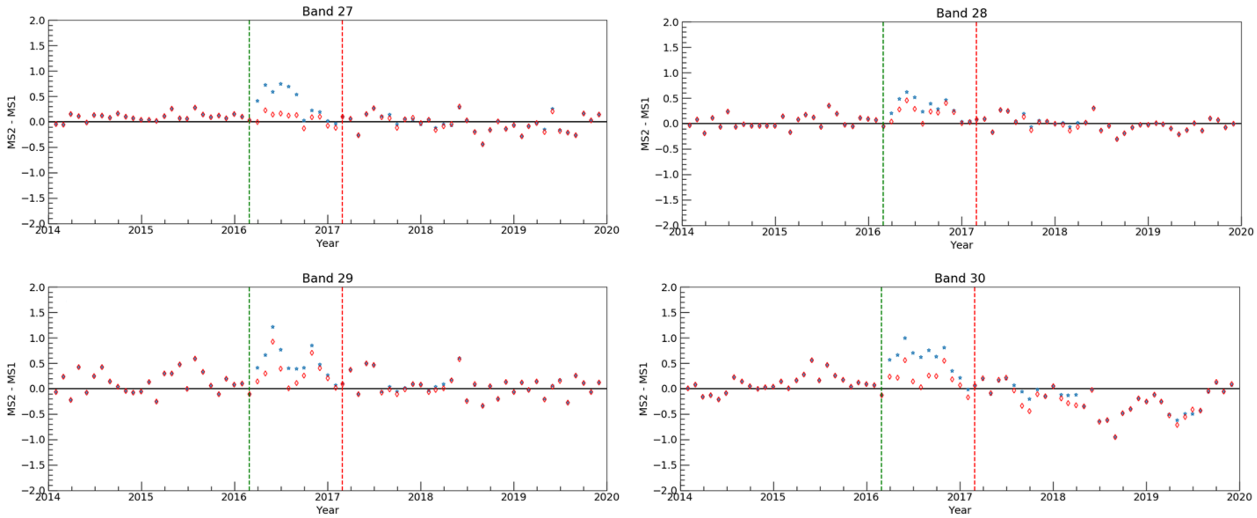

Figure 4. Terra PV LWIR 27-30 mirror side BT differences in Kevin from 2014 to 2020 over Dome-C. Each symbol defines the monthly- and band-averaged value. The blue stars represent C6.1, while the red diamonds indicate future improvements. The vertical dashed lines indicate the time of occurrence for safe mode (February 2016) and one year after the event.

Table 2. Terra DCC mirror side BT differences for the same month (March 2016) using official C6.1 and the future improvements Collection.

Band	C6.1 DCC BT (K) 03/2016	C6.1 MS BT diff.(K) 03/2016	Test LUT DCC BT (K) 03/2016	Test LUT MS BT diff.(K) 03/2016
20	202.3	-0.180	202.3	0.061
22	200.9	-0.353	200.9	-0.180
23	200.6	-0.367	200.6	-0.138
24	207.9	-0.194	207.9	-0.162
25	202.5	-0.228	202.5	-0.109
27	200.3	1.582	200.4	0.478
28	200.0	0.599	200.1	0.092
29	200.5	0.747	200.6	0.232
30	210.2	0.570	210.4	-0.038
32	198.5	-0.013	198.5	-0.014
33	200.3	-0.027	200.3	-0.025
34	201.5	0.085	201.5	0.094
35	203.7	-0.072	203.7	-0.076
36	204.3	-0.147	204.8	-0.216

3.3 Aqua MODIS

3.3.1 Aqua mirror side difference

In January 2018, Aqua MODIS underwent a configuration change attributed to its B-side electronic formatter resetting. Electronic setting changes can cause mirror side correlated noise and mirror side difference changes, as seen early in the Terra mission. Since the formatter reset only caused a few digital output number changes, its impact is not noticeable over typical (or higher) radiance scenes. However, assessments using cold targets (e.g. DCC and Dome-C) can reveal the effect of this event[14, 21]. Figure 5 shows the mirror side radiance and BT differences for MWIR bands 20-25. As mentioned in Sec. 3.2, the radiance difference is used for offset term bias assessments. Band 20 has the largest mirror side BT difference (approximately 1.8 K relative radiance difference) before the formatter reset. After the reset, this mirror side difference is significantly reduced (dropping to 0.5 K relative radiance). The other MWIR TEB also show up to a 1 K mirror side BT difference before the formatter reset event. Because TEB 21 uses a linear calibration algorithm, its mirror side BT differences are not directly comparable to the other bands. Before and after the formatter reset, the TEB 21 mirror side BT differences change direction. For all other TEB, the mirror side differences are smaller after the reset.

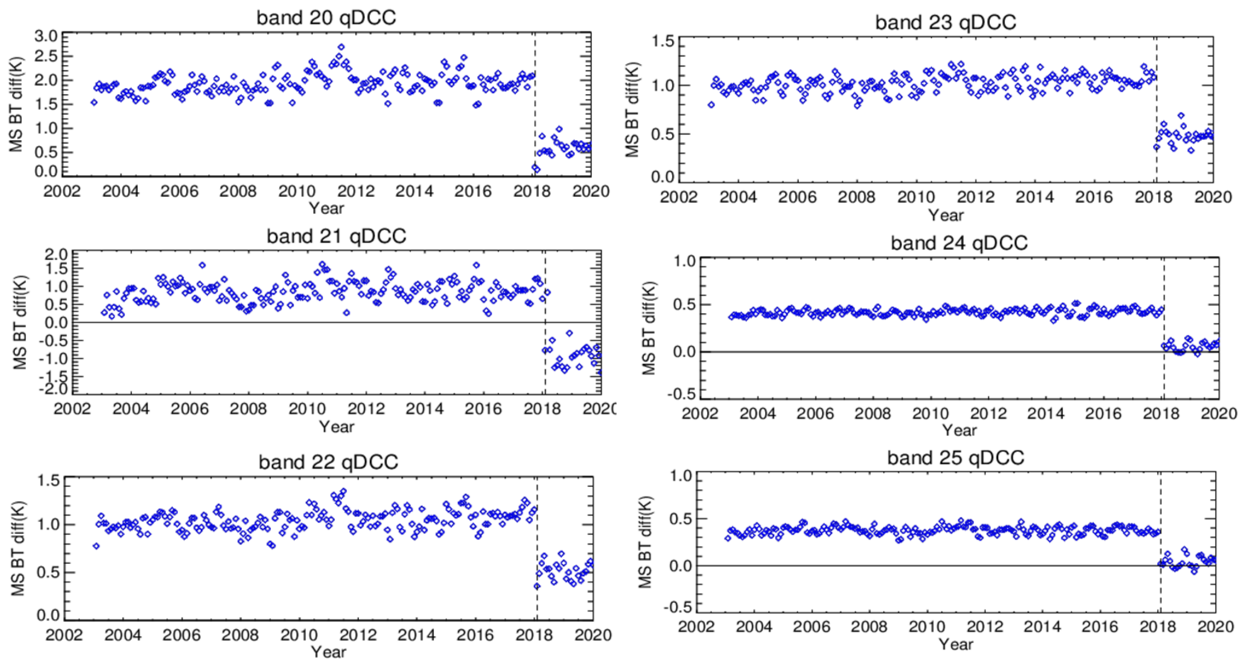

Figure 5. Aqua MWIR bands 20-25 mirror side BT differences long-term trending using qDCC. Each symbol represents monthly-averaged mirror side differences. The vertical dashed line indicates the time of occurrence for the formatter reset (January 2018).

Figure 6 shows the mirror side radiance and BT differences for PV LWIR bands 27-30. Band 27 has the largest mirror side difference among these four bands (approximately 0.8 K) before the formatter reset. Similarly to the MWIR TEB, after the reset, the mirror side differences for all four bands significantly decreased. Moreover, all four bands exhibit slight - and similar in pattern - mirror side difference fluctuations, suggesting that these are not noise. The PC LWIR TEB mirror side differences are negligible and not shown here.

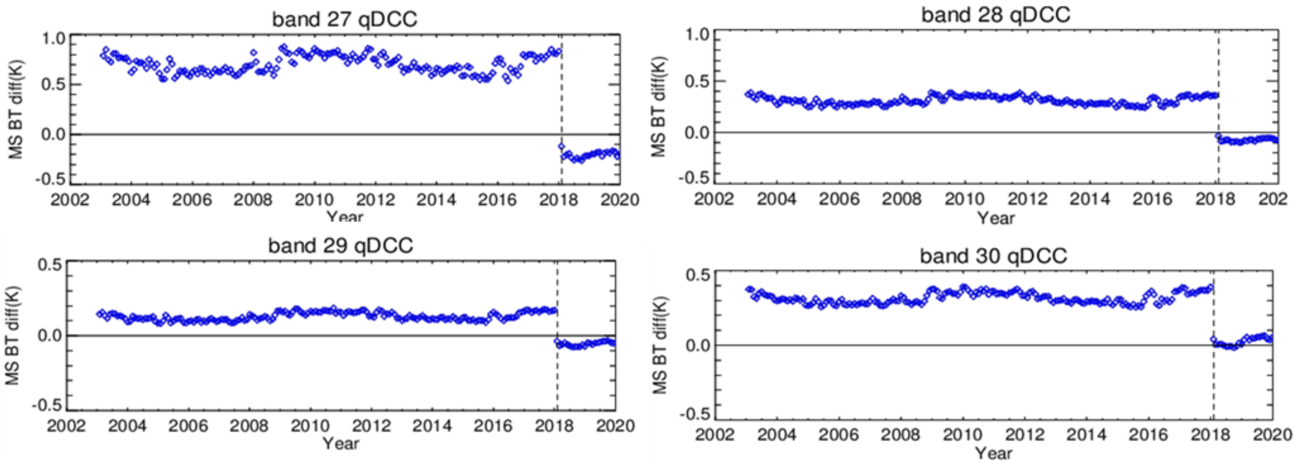

Figure 6. Aqua LWIR bands 27-30 mirror side BT differences long-term trending using qDCC. Each symbol represents monthly-averaged mirror side differences. The vertical dashed line indicates the time of occurrence for the formatter reset (January 2018).

3.3.2 Aqua MODIS calibration improvement

As presented in Sec. 4.2, the Aqua TEB mirror side BT differences are also assessed using DCC measurements. Aqua MODIS mirror side differences were affected by the formatter reset on January 2018. An analytical model was developed to derive the a_0 relative mirror side bias using DCC assessments. Using the bias from each month over DCC, a correction for the offset coefficient can be derived. An algorithm improvement is proposed and tested in which the pre-launch $a_0$is corrected and $a_2$is derived from the CD data[30].

Selected EV measurements were reprocessed using this algorithm. Figure 7 shows the C6.1 product and LUT improvement test mirror side BT differences for Aqua TEB 22, 23, 27, and 30. The Aqua measurements are analyzed using a MODIS-to-AIRS comparison. The MODIS and AIRS instruments are both onboard the Aqua spacecraft. The data shown are from September 17, 2017. Results indicate a significant reduction in mirror side differences for the chosen bands. All other bands covered by the AIRS spectrum show significant improvement as well. The test L1B data were generated using two months of DCC data (one month before and one month after the formatter reset). The test results show significant improvement (Table 3). In C6.1, the mirror side differences for the MWIR bands - especially TEB 20, 22, and 23 - are relative large. After the correction, these are largely reduced. For PV LWIR TEB 27-30, the biases are also substantial before the correction and reduced after. The biases for the PC LWIR bands are minor and the correction further reduces them.

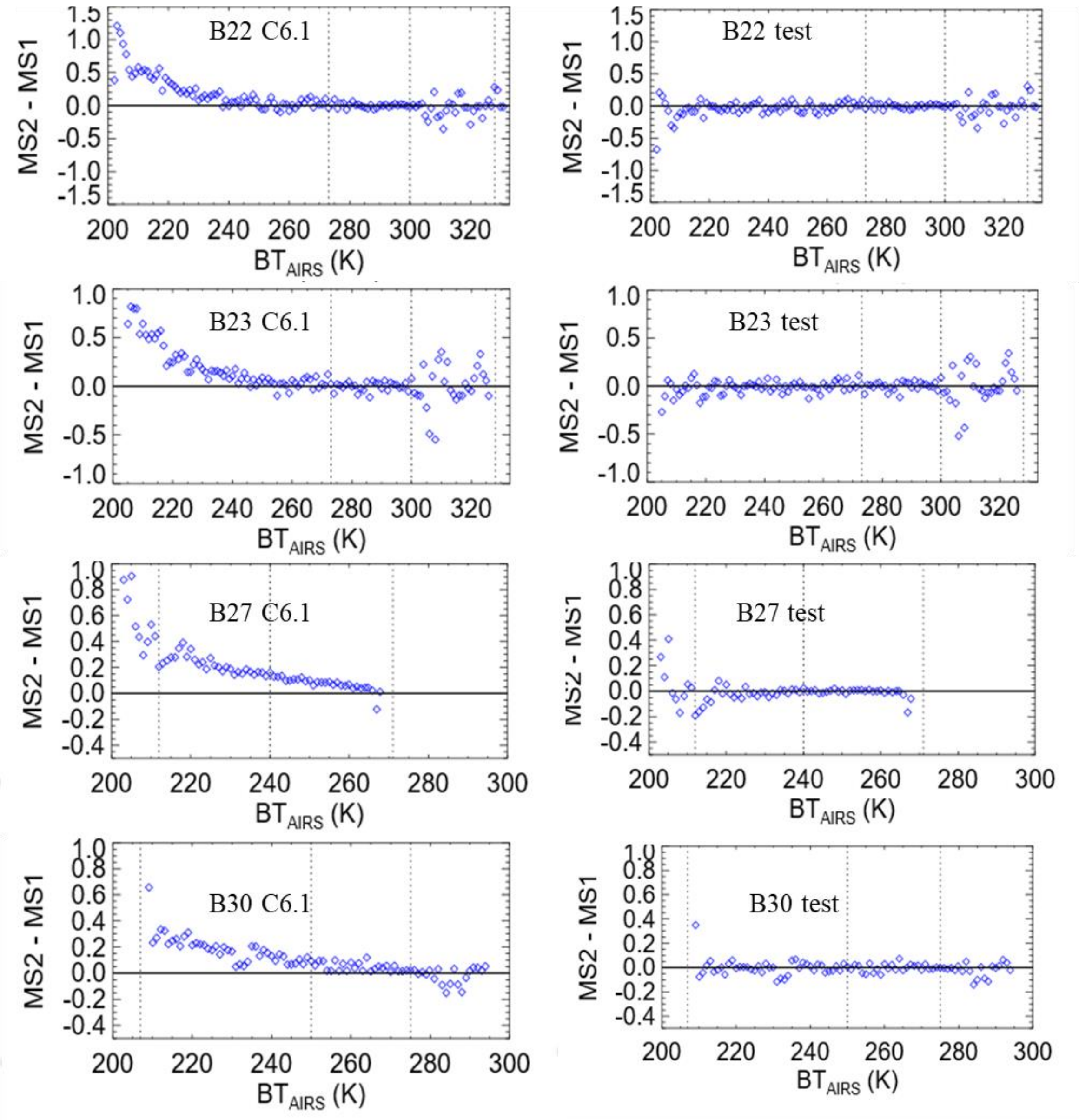

Figure 7. Aqua C6.1 product and LUT improvement test mirror side BT differences in Kevin for Aqua TEB 22, 23, 27, and 30 using an Aqua MODIS-to-AIRS comparison. All data shown are from September 17, 2017. (Left) C6.1 mirror side BT differences as a function of the AIRS BT for Aqua bands 22, 23, 27, and 30. (Right) Test LUT mirror side BT differences as a function of the AIRS BT for Aqua bands 22, 23, 27, and 30. The vertical dotted lines represent BTs at 0.3 of typical radiance, typical temperature, and maximum temperature for each TEB from left to right, respectively.

Table 3. Aqua C6.1 and test LUT mirror side BT differences one month before and one month after the Aqua formatter reset over DCC measurements.

Band	C6.1 qDCC BT (K) 07/2017	C6.1 MS BT diff.(K) 07/2017	Test LUT MS BT diff.(K) 07/2017	C6.1 MS BT diff.(K) 07/2018	Test LUT MS BT diff.(K) 07/2018
20	202.9	1.845	0.168	0.474	-0.252
22	203.5	1.227	0.042	0.514	-0.208
23	204.0	1.076	-0.045	0.456	-0.190
24	209.0	0.264	0.008	0.005	-0.068
25	205.0	0.385	0.015	-0.006	-0.120
27	199.5	0.978	-0.021	-0.284	-0.046
28	200.2	0.428	-0.005	-0.100	-0.016
29	200.9	0.192	-0.007	-0.083	-0.029
30	211.1	0.392	0.010	0.014	0.013
32	198.9	-0.029	0.002	-0.035	-0.007
33	201.2	-0.038	0.007	-0.048	-0.017
34	202.9	-0.022	0.003	-0.026	0.001
35	205.3	0.009	-0.005	-0.015	0.005
36	206.7	-0.011	0.004	-0.026	-0.007

4. SUMMARY

Measurements over various Earth scenes are used for sensor calibration assessments. Moreover, colder scenes (i.e. DCC and Dome-C) are utilized for the assessment of the offset coefficient in the calibration algorithm. Mirror side differences are analyzed over the entire Terra and Aqua MODIS missions for the TEB. The Terra safe mode event had an impact on the C6.1 LUT due to the one-year moving averaging, thus affecting the calibrated L1B products. Biases over the DCC/qDCC measurements revealed that when the yearly moving average window is used to produce the TEB calibration LUT across the safe mode timeline, it has noticeable impacts on the PV LWIR TEB calibrated product. A correction procedure has been proposed and tested. The Aqua MODIS TEB mirror side differences over its entire mission were also analyzed using DCC/qDCC measurements. By applying an analytical model, an algorithm for the correction of the Aqua MODIS TEB calibration offset coefficients has been proposed and tested. The Aqua MODIS formatter reset from January 2018 impacted the TEB mirror side differences. Before the reset, the mirror side differences were significantly large, especially for some of the PV bands (i.e. TEB 20, 22, 23, and 27). After the event, mirror side differences became smaller. After testing the proposed correction, mirror side difference improvements before and after the formatter reset were demonstrated.

These calibration improvements have been tested using a simulation tool and were verified using various Earth scenes (e.g. desert, ocean), as well as a comparison with a reference sensor (MODIS-to-AIRS comparison). The verification using Earth measurements was also validated by the analytical model. The changes due to the algorithm improvements for warm scenes are insignificant for both instruments. These improvements have been recommended to be implemented in the future Collection of the L1B.

ACKNOWLEDGMENTS

The authors would like to thank Amit Angal for the internal reviews performed on this manuscript. The authors would also like to thank other members of the MODIS Characterization Support Team for their technical assistance and contributions.

REFERENCES

[1] W. L. Barnes and V. V. Salomonson, “MODIS: A global image spectroradiometer for the Earth Observing System,” Crit. Rev. Opt. Sci. Technol., vol. CR47, 285–307, 1993.

[2] W. L. Barnes, V. V. Salomonson, B. Guenther, and X. Xiong, “Development, characterization, and performance of the EOS MODIS sensors,” in Proc. SPIE, 5151, 337–345, 2003.

[3] W. L. Barnes, X. Xiong, and V. V. Salomonson, “Status of Terra MODIS and Aqua MODIS,” J. Adv. Space Res., 32(11), 2099–2106, 2003.

[4] V. V. Salomonson, W. L. Barnes, X. Xiong, S. Kempler, and E. Masuoka, “An overview of the Earth Observing System MODIS instrument and associated data systems performance,” in Proc. IEEE IGARSS, 1174–1176, 2002.

[5] C. L. Parkinson, "Summarizing the first ten years of NASA's Aqua mission", IEEE J. Sel. Topics Appl. Earth Observ. Remote Sens., 6(3), 1179-1188, 2013.

[6] Yue, H., C. He, Y. Zhao, Q. Ma; Q. Zhang, “The brightness temperature adjusted dust index: An improved approach to detect dust storms using MODIS imagery”. INTERNATIONAL JOURNAL OF APPLIED EARTH OBSERVATION AND GEOINFORMATION, 57, 166-176, 2017.

[7] Skakun, S., CO Justice, E Vermote, JC Roger Transitioning from MODIS to VIIRS: an analysis of inter-consistency of NDVI data sets for agricultural monitoring” International journal of remote sensing, 39(4), 971-992, 2018

[8] Gupta, Pawan; Remer, Lorraine A; Levy, Robert C; Mattoo, Shana, “Validation of MODIS 3 km land aerosol optical depth from NASA's EOS Terra and Aqua missions” Atmospheric Measurement Techniques; Katlenburg-Lindau 11 (5), 2018

[9] R. C. Levy, S. Mattoo, L. A. Munchak, L. A. Remer, A. M. Sayer, F. Patadia, and N. C. Hsu, “The Collection 6 MODIS aerosol products over land and ocean”, Atmos. Meas. Tech., 6, 2989–3034, 2013

[10] Wilson, T., A. Wu, A.. Shrestha, X. Geng, Z. Wang, C. Moeller, R. Frey, and X. Xiong, "Development and Implementation of an Electronic Crosstalk Correction for Bands 27–30 in Terra MODIS Collection 6", Remote Sensing, vol. 9(6), issue 569, 2017

[11] Xiong, X., B. Wenny, A. Wu, and V. Salomonson, "Aqua MODIS Thermal Emissive Bands On-orbit Calibration, Characterization, and Performance", IEEE Trans. Geosci. Remote Sens., vol. 47, issue 3, pp. 803-814, 2009

[12] Xiong, X., A. Wu, B. N. Wenny, S. Madhavan, Z. Wang, Y. Li, N. Chen, W. Barnes, and V. Salomonson, "Terra and Aqua MODIS Thermal Emissive Bands On-Orbit Calibration and Performance", IEEE Transactions on Geoscience and Remote Sensing, vol. 53, issue 10, pp. 5709 - 5721, 2015.

[13] Chang, T., X. Xiong, A. Shrestha, A. Wu, N. Chen, Y. Li, and Q. Mu, "Assessment of Terra MODIS thermal emissive band calibration using cold targets and measurements in lunar roll events", Proc. SPIE - Sensors, Systems, and Next-Generation Satellites XXII, vol. 10785, pp. 107851C, 2018.

[14] Chang, T., X. Xiong, A. Angal, and Q. Mu, "Assessment of MODIS RSB detector uniformity using deep convective clouds", Journal of Geophysical Research: Atmospheres, vol. 121, issue 9, pp. 4783–4796, 2016

[15] Xiong, X., A. Wu, and B. Wenny, "Using Dome C for MODIS Calibration Stability and Consistency", J. Appl. Remote Sens., vol. 3, no. 033520, 2009.

[16] Cao, C., S. Uprety, X. Xiong, A. Wu, P. Jing, D. Smith, G. Chander, N. Fox, and S. Ungar, "Establishing the Antarctic Dome C Community Reference Standard Site towards Consistent Measurements from Earth Observation Satellites", Canadian Journal of Remote Sensing , vol. 36, issue 5, 2010

[17] Wenny, B., and X. Xiong, "Using a Cold Earth Surface Target to Characterize Long-term Stability of the MODIS Thermal Emissive Bands", IEEE Geosci. Remote Sens. Let., vol. 5, issue 2, pp. 162-165, 2008

[18] Doelling, D. R., L. Nguyen, P. Minnis (2004), On the use of deep convective clouds to calibrate AVHRR data, in Proc. SPIE, Earth Observing Systems IX, pp. 281-299

[19] Doelling, D.R., G. Hong, D. Morstad, R. Bhatt, A. Gopalan, and X. Xiong (2010), The Characterization of Deep Convective Cloud Albedo as a Calibration Target Using MODIS Reflectances, in Proc. SPIE, Earth Observing Missions and Sensors: Development, Implementation, and Characterization, vol. 7862, 78620I-1 to 78620I-10

[20] Mu, Q., A. Wu, X. Xiong, D. R. Doelling, A. Angal, T. Chang, and R. Bhatt, "Optimization of a Deep Convective Cloud Technique in Evaluating the Long-Term Radiometric Stability of MODIS Reflective Solar Bands", Remote Sensing, vol. 9 (6), issue 535, 2017

[21] Chang, T., X. Xiong, A. Shrestha, and P. C. Diaz, "Methodology development for calibration assessment using quasi-deep convective clouds with application to Aqua MODIS TEB", Earth and Space Science, vol. 7, issue 1, pp. 1-15, 2020

[22] C. Diaz, P., X. Xiong, and A. Wu, "MODIS thermal emissive bands calibration stability using in-situ ocean targets and remotely-sensed SST retrievals provided by the group for high resolution sea surface temperature", Proc. SPIE 11014, Ocean Sensing and Monitoring XI, vol. 110140, pp. 110140P, 2019.

[23] Shrestha, A., A. Wu, and X. Xiong, "Evaluating calibration consistency of Terra and Aqua MODIS LWIR PV bands using Dome C", Proc. SPIE", 10644, 106440N (2018)

[24] Xiong, X., A. Wu, and B. Wenny, "Using Dome C for MODIS Calibration Stability and Consistency", J. Appl. Remote Sens., vol. 3, no. 033520, 2009.

[25] Cao, C., S. Uprety, X. Xiong, A. Wu, P. Jing, D. Smith, G. Chander, N. Fox, and S. Ungar, "Establishing the Antarctic Dome C Community Reference Standard Site towards Consistent Measurements from Earth Observation Satellites", Canadian Journal of Remote Sensing , vol. 36, issue 5, 2010

[26] Wenny, B., and X. Xiong, "Using a Cold Earth Surface Target to Characterize Long-term Stability of the MODIS Thermal Emissive Bands", IEEE Geosci. Remote Sens. Let., vol. 5, issue 2, pp. 162-165, 2008

[27] Xiong, X., A. Angal, A. Wu, D. Link, X. Geng, W. Barnes, and V. Salomonson, "Sixteen years of Terra MODIS on-orbit operation, calibration, and performance ", Proc. SPIE 10000, Sensors, Systems, and Next-Generation Satellites XX, 100000V, (2016)

[28] Chang, T., Xiong, X. and Shrestha, A., "Assessment of MODIS thermal emissive bands calibration performance using deep convective clouds," JARS 13(4), 044526 (2019).

[29] Xiong, X., E. Aldoretta, A. Angal, T. Chang, and X. Geng, "Terra MODIS: 20 years of on-orbit calibration and performance", Proc. SPIE 11127, Earth Observing Systems XXIV, vol. 11127, pp. 1112714, (2019)

[30] Wu, A., X. Xiong, B. Wenny, C. Moeller, N. Che, and K. Chiang, "Improvement of low temperature estimation for MODIS thermal emissive bands by adjusting calibration offset and nonlinear terms, Earth Observing Systems XII", Proc. SPIE, vol. 6677, no. 66771H, 2007.